

1 **Interpreting UniFrac with Absolute Abundance: A Conceptual and Practical Guide**

2 Augustus Pendleton^{1*} & Marian L. Schmidt^{1*}

3 ¹Department of Microbiology, Cornell University, 123 Wing Dr, Ithaca, NY 14850, USA

4 **Corresponding Authors:** Augustus Pendleton: arp277@cornell.edu; Marian L. Schmidt:
5 marschmi@cornell.edu

6 **Author Contribution Statement:** Both authors contributed equally to the manuscript.

7 **Preprint servers:** This article was submitted to *bioRxiv* (doi: 10.1101/2025.07.18.665540) under
8 a CC-BY-NC-ND 4.0 International license.

9 **Keywords:** Microbial Ecology - Beta Diversity - Absolute Abundance - Bioinformatics -
10 UniFrac

11 **Data Availability:** All data and code used to produce the manuscript are available at
12 https://github.com/MarschmiLab/Pendleton_2025_Absolute_Unifrac_Paper, in addition to a
13 reproducible renv environment. All packages used for analysis are listed in Table S1.

14

15 **Abstract**

16 β -diversity is central to microbial ecology, yet commonly used metrics overlook changes in
17 microbial load (or “absolute abundance”), limiting their ability to detect ecologically meaningful
18 shifts. Popular for incorporating phylogenetic relationships, UniFrac distances currently default
19 to relative abundance and therefore omit important variation in microbial abundances. As
20 quantifying absolute abundance becomes more accessible, integrating this information into β -
21 diversity analyses is essential. Here, we introduce *Absolute UniFrac* (U^A), a variant of Weighted
22 UniFrac that incorporates absolute abundances. Using simulations and a reanalysis of four 16S
23 rRNA metabarcoding datasets (from a nuclear reactor cooling tank, the mouse gut, a freshwater
24 lake, and the peanut rhizosphere), we demonstrate that Absolute UniFrac captures microbial load,
25 composition, and phylogenetic relationships. While this can improve statistical power to detect
26 ecological shifts, we also find Absolute UniFrac can be strongly correlated to differences in cell
27 abundances alone. To balance these effects, we also incorporate absolute abundance into the
28 generalized extension (GU^A) that has a tunable, continuous ecological parameter (α) that
29 modulates the relative contribution of rare versus abundant lineages to β -diversity calculations.
30 Finally, we benchmark GU^A and show that although computationally slower than conventional
31 alternatives, GU^A is comparably sensitive to noise in load estimates compared to conventional
32 alternatives like Bray-Curtis dissimilarities, particularly at lower α . By coupling phylogeny,
33 composition, and microbial load, Absolute UniFrac integrates three dimensions of ecological
34 change, better equipping microbial ecologists to quantitatively compare microbial communities.

Deleted: that has a tunable α parameter to adjust the influence of abundance and composition.

Deleted: in

Deleted: realistic

39 **Main Text**

40 Microbial ecologists routinely compare communities using β -diversity metrics derived
41 from relative abundances. Yet this approach overlooks a critical ecological dimension: microbial
42 load. High-throughput sequencing produces compositional data, in which each taxon's
43 abundance is constrained by all others [1]. However, quantitative profiling studies show that cell
44 abundance, not only composition, can drive major community differences [2]. In low-biomass
45 samples, relying on relative abundance can allow contaminants to appear biologically
46 meaningful despite absolute counts too low for concern [3].

47 Sequencing-based microbiome studies therefore rely on relative abundance even when
48 the hypotheses of interest implicitly concern absolute changes in biomass. This creates a
49 mismatch between ecological framing (growth, bloom magnitude, pathogen proliferation,
50 disturbance recovery, or colonization pressure) and the information the β -diversity metric
51 encodes [4]. As a result, β -diversity is often treated as if it includes biomass, even when absolute
52 abundance is either not measured at all or is measured but excluded from the calculation (as in
53 conventional UniFrac). Many studies therefore test biomass-linked hypotheses using a metric
54 that normalizes biomass away [4]. A conceptual correction is needed in which β -diversity is
55 understood as variation along three axes: composition, phylogeny and absolute abundance.

56 Absolute microbial load measurements are now increasingly obtainable through flow
57 cytometry, qPCR, and genomic spike-ins, allowing biomass to be quantified alongside taxonomic
58 composition [4, 5]. These approaches improve detection of functionally relevant taxa and
59 mitigate the compositional constraints imposed by sequencing [1, 2]. Most studies that
60 incorporate absolute abundance counts currently rely on Bray-Curtis dissimilarity, which can
61 capture load but does not consider phylogenetic similarity [5–7]. Unifrac distances provide the
62 opposite strength, incorporating phylogeny but discarding absolute abundance, as they are
63 restricted to relative abundance data by construction [8]. This leaves no phylogenetically
64 informed β -diversity metric that operates on absolute counts, despite the fact that biomass is
65 central to many ecological hypotheses.

66 To evaluate the implications of incorporating absolute abundance into phylogenetic β -
67 diversity, we use both simulations and reanalysis of four 16S rRNA amplicon datasets. The
68 simulations use a simple four-taxon community with controlled abundance shifts to directly
69 compare both Bray-Curtis and UniFrac in their relative and absolute forms, illustrating how each
70 metric responds when abundance, composition, or evolutionary relatedness differ. We then
71 reanalyze four real-world datasets spanning nuclear reactor cooling water [5], the mouse gut [3],
72 a freshwater lake [9], and rhizosphere soil [10]. These differ widely in richness, biomass range,
73 and ecological context, allowing us to test when absolute abundance changes align with or
74 diverge from phylogenetic turnover. Together, these simulations and reanalyses provide the
75 empirical foundation for interpreting Absolute UniFrac relative to existing β -diversity measures
76 across the three axes of ecological difference: abundance, composition, and phylogeny.

77 We also extend Absolute UniFrac as was proposed by [11] to Generalized Absolute
78 UniFrac that incorporates a tunable ecological dimension, α , and evaluate its impact across
79 simulated and real-world datasets. As α increases, β -diversity is increasingly correlated with
80 differences in absolute abundance, allowing researchers to fine tune the relative weight their
81 analyses place on microbial load versus composition.

82 **Defining Absolute UniFrac**

83 The UniFrac distance was first introduced by Lozupone & Knight (2005) and has since
 84 become enormously popular as a measure of β -diversity within the field of microbial ecology
 85 [12]. A benefit of the UniFrac distance is that it considers phylogenetic information when
 86 estimating the distance between two communities. After first generating a phylogenetic tree
 87 representing species (or amplicon sequence variants, “ASVs”) from all samples, the UniFrac
 88 distance computes the fraction of branch-lengths which is *shared* between communities, relative
 89 to the total branch length represented in the tree. UniFrac can be both unweighted, in which only
 90 the incidence of species is considered, or weighted, wherein a branch’s contribution is weighted
 91 by the proportional abundance of taxa on that branch [8]. The Weighted UniFrac is derived:

$$92 \quad U^R = \frac{\sum_{i=1}^n b_i |p_i^a - p_i^b|}{\sum_{i=1}^n b_i (p_i^a + p_i^b)}$$

93 where the contribution of each branch length, b_i , is weighted by the difference in the relative
 94 abundance of all species (p_i) descended from that branch in sample a or sample b . Here, we
 95 denote this distance as U^R , for “Relative UniFrac”. Popular packages which calculate weighted
 96 UniFrac—including the diversity-lib QIIME plug-in and the R packages phyloseq and
 97 GUniFrac—run this normalization by default [11, 13, 14].

98 Importantly, U^R is most sensitive to changes in abundant lineages, which can sometimes
 99 obscure compositional differences driven by rare to moderately-abundant taxa [11]. To address
 100 this weakness, Chen et al. (2012) introduced the generalized UniFrac distance (GU^R), in which
 101 the impact of abundant lineages can be mitigated by decreasing the parameter α :

$$102 \quad GU^R = \frac{\sum_{i=1}^n b_i (p_i^a + p_i^b)^\alpha |p_i^a - p_i^b|}{\sum_{i=1}^n b_i (p_i^a + p_i^b)^\alpha}$$

103 where α ranges from 0 (close to Unweighted UniFrac) up to 1 (identical to U^R , above). However,
 104 if one wishes to use absolute abundances, both U^R and GU^R can be derived without normalizing
 105 to proportions:

$$106 \quad U^A = \frac{\sum_{i=1}^n b_i |c_i^a - c_i^b|}{\sum_{i=1}^n b_i (c_i^a + c_i^b)} \quad GU^A = \frac{\sum_{i=1}^n b_i (c_i^a + c_i^b)^\alpha |c_i^a - c_i^b|}{\sum_{i=1}^n b_i (c_i^a + c_i^b)^\alpha}$$

107 Where c_i^a and c_i^b denote for the absolute counts of species descending from branch b_i in
 108 communities a and b , respectively. We refer to these distances as *Absolute UniFrac* (U^A) and
 109 *Generalized Absolute UniFrac* (GU^A). Although substituting absolute for relative abundances is
 110 mathematically straightforward, to our knowledge there is no prior work that examines UniFrac
 111 in the context of absolute abundance, either conceptually or in application. Incorporating
 112 absolute abundances introduces a third axis of ecological variation: beyond differences in
 113 composition and phylogenetic similarity, U^A also captures divergence in microbial load. This
 114 makes interpretation of U^A nontrivial, particularly in complex microbiomes.

Deleted: we found

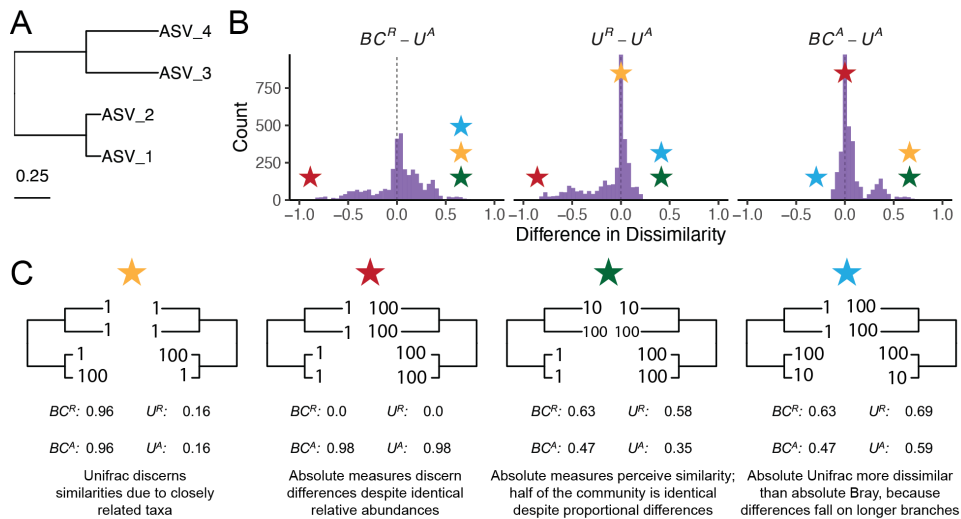
115 **Demonstrating β -diversity metrics’ behavior with a simple simulation**

117 To clarify how U^A behaves relative to existing β -diversity metrics, we first constructed a
118 simple four-taxon simulated community arranged in a small phylogeny (Fig. 1A). By varying the
119 absolute abundance of each ASV (1, 10, or 100), we generated 81 samples and 3,240 pairwise
120 comparisons. For each pair, we computed four dissimilarity metrics: Bray-Curtis with relative
121 abundance (BC^R), Bray-Curtis with absolute abundance (BC^A), Weighted UniFrac with relative
122 abundance (U^R), and Weighted UniFrac with absolute abundance (U^A). These comparisons help
123 to illustrate how each axis of ecological difference—abundance, composition, and phylogeny—is
124 expressed by the different metrics.

125 U^A does not consistently yield higher or lower distances compared to other metrics, but
126 instead varies depending on how abundance and phylogeny intersect (Fig. 1B). In the improbable
127 scenario that all branch lengths are equal, U^A is always less than or equal to BC^A (Fig. S1).
128 These comparisons emphasize that once branch lengths differ, incorporating phylogeny and
129 absolute abundance alters the structure of the distance space. The direction and magnitude of that
130 change depend on which branches carry the abundance shifts. U^A is also usually smaller than
131 BC^A and is more strongly correlated with BC^A (Pearson's $r = 0.82$, $p < 0.0001$) than with BC^R (r
132 = 0.41) and U^R ($r = 0.55$).

133 To better understand how these metrics diverge, we examined individual sample pairs
134 (Fig. 1C). Scenario 1 (gold star) illustrates the classic advantage of UniFrac: ASV_1 and ASV_2
135 are phylogenetically close, so U^R and U^A discern greater similarity between samples than BC^R
136 and BC^A , which ignore phylogenetic structure. Scenario 2 (red star) highlights a limitation of
137 relative metrics: two samples with identical relative composition but a 100-fold difference in
138 biomass appear identical to BC^R and U^R , but not to their absolute counterparts. In Scenario 3
139 (green star), incorporating absolute abundance decreases dissimilarity. BC^A and U^A are lower
140 than their relative counterparts because half the community is identical in absolute abundance,
141 even though their proportions differ. In contrast, Scenario 4 (blue star) shows that U^A can exceed
142 BC^A when abundance differences occur on long branches, amplifying phylogenetic dissimilarity.

143 These scenarios demonstrate that U^A integrates variation along three ecologically
144 relevant axes: composition, phylogenetic similarity, and microbial load, rather than isolating any
145 single dimension. Because a given U^A value can reflect multiple drivers of community change,
146 interpreting it requires downstream analyses to disentangle the relative contributions of these
147 three axes. To evaluate how this plays out in real systems we next reanalyzed four previously
148 published datasets spanning diverse microbial environments.

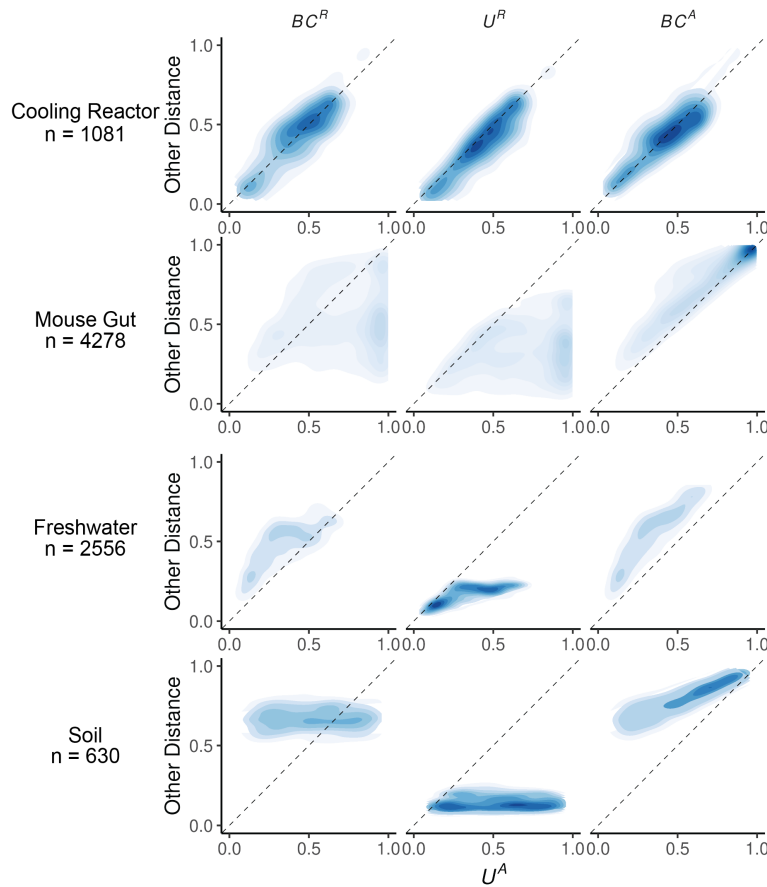


152 *Figure 1. Simulated communities reveal how absolute abundance affects phylogenetic and non-phylogenetic β -*
153 *diversity measures.* (A) We constructed a simple four-ASV community with a known phylogeny and generated all
154 permutations of each ASV having an absolute abundance of 1, 10, or 100, resulting in 81 unique communities and
155 3,240 pairwise comparisons. (B) Distributions of pairwise differences between weighted UniFrac using absolute
156 abundance (U^A) and three other metrics: Bray-Curtis using relative abundance (BC^R), weighted UniFrac using
157 relative abundance (U^R), and Bray-Curtis using absolute abundance (BC^A). (C) Illustrative sample pairs demonstrate
158 how absolute abundances and phylogenetic structure interact to increase or decrease dissimilarity across metrics.
159 Stars indicate where each scenario falls within the distributions shown in panel B. Actual values for each metric are
160 displayed beneath each scenario.

161 Application of Absolute UniFrac to Four Real-World Microbiome Datasets

162 To illustrate the sensitivity of U^A to both variation in composition and absolute
163 abundance, we re-analyzed four previously published datasets from diverse microbial systems.
164 These datasets included: (i) nuclear reactor cooling water sampled across three reactor cycle
165 phases [5]; (ii) the mouse gut sampled across multiple regions and between two diets [3]; (iii)
166 depth-stratified freshwater communities sampled across two months [9]; and (iv) peanut
167 rhizospheres under two crop rotation schemes (conventional rotation (CR) vs. sod-based rotation
168 (SBR)), plant maturities, and irrigation treatments [10]. Absolute abundance was quantified by
169 flow cytometry for the cooling water and freshwater datasets, droplet digital PCR for the mouse
170 gut, and by qPCR for the rhizosphere dataset. Together these span a wide range of richness—from
171 215 ASVs in the cooling water to 24,000 ASVs in the soil—and microbial load—from as low as
172 4×10^5 cells/ml (cooling water) up to 2×10^{12} 16S rRNA copies/gram (mouse gut). Additional

173 details of the re-analysis workflow, including ASV generation and phylogenetic inference, are
 174 provided in the Supporting Methods.



175 *Figure 2. Absolute UniFrac (U^A) compared with other β -diversity metrics across four real microbial datasets.* Each
 176 panel shows pairwise sample distances for U^A (x-axis) against another metric (y-axis): Bray-Curtis using relative
 177 abundance (BC^R , first column), weighted UniFrac using relative abundances (U^R , second column), and Bray-Curtis
 178 using absolute abundances (BC^A , third column). Contours indicate the relative density of pairwise comparisons (n
 179 shown for each dataset, left), with darker shading corresponding to more observations. The dashed line marks the
 180 1:1 relationship. Points above the line indicate cases where U^A is smaller than the comparator metric, while points
 181 below the line indicate cases where U^A is larger.

182 We first calculated four β -diversity metrics for all sample pairs in each dataset and
 183 compared them to U^A (Fig. 2). The degree of concordance between U^A and other metrics was
 184 highly context dependent. In the cooling water dataset, U^A closely tracked all three alternatives,
 185 whereas in the remaining systems it diverged substantially. U^A also spanned a similar or wider

186 range of distances than the other metrics. For example, in the soil dataset BC^R and U^R occupied a
187 narrow range relative to the broad separation observed under U^A .

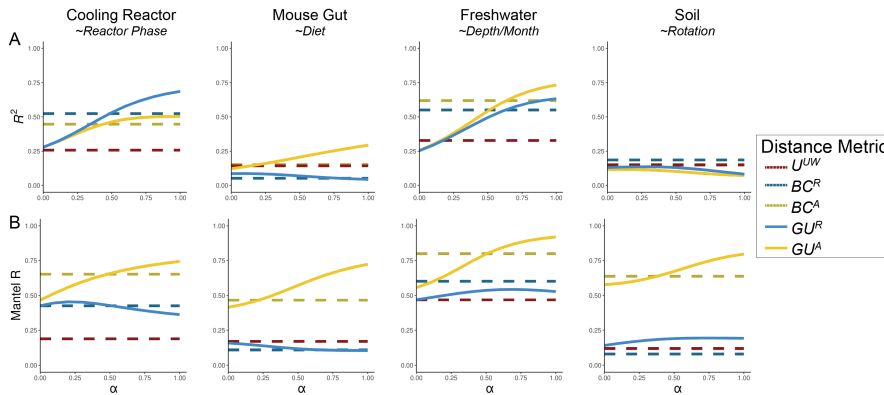
188 U^A generally reported distances that were similar to or greater than U^R , consistent with
189 the simulations shown in Fig. 1B. This reflects the ability of U^A to discern dissimilarity due to
190 differences in microbial load, even when community composition is conserved. In contrast, U^A
191 yielded distances that were similar to or lower than BC^A , again matching the simulated behavior
192 in Fig 1B. In these cases, phylogenetic proximity between abundant, closely-related ASVs leads
193 to register greater similarity than BC^A .

194 Given these differences, we next quantified how well each metric discriminates among
195 categorical sample groups. For each dataset, we ran PERMANOVAs to measure the proportion
196 of variance (R^2) and statistical power (*pseudo-F*, *p*-value) attributable to group structure, using
197 groupings that were determined to be significant in the original publications. To evaluate how
198 strongly absolute abundance contributed to this discrimination, we also calculated GU^A across a
199 range of α values. The resulting R^2 values are displayed in Fig. 3A, with the corresponding
200 *pseudo-F* statistics and *p*-values provided in Fig. S2.

201 As in Fig. 2, the performance of each metric was strongly context dependent (Fig. 3A). In the
202 mouse gut and freshwater datasets, absolute-abundance-aware metrics (BC^A and GU^A) explained
203 the greatest proportion of variance (R^2), and R^2 generally increasing as α increased. In contrast,
204 relative metrics captured more variation in the cooling water dataset (again at higher α), and all
205 metrics explained comparably little variance in the soil dataset. Taken at face value, these trends
206 might suggest that higher α values typically improve group differentiation.

207 However, this comes with a major caveat: at high α values, GU^A becomes strongly
208 correlated with total cell count alone (Fig. 3B). Mantel tests confirmed that absolute-abundance
209 metrics are far more sensitive to differences in microbial load than their relative counterparts.
210 This behavior is intuitive, and to some extent desirable, because these metrics are designed to
211 detect changes in microbial load even when composition remains constant. Yet at $\alpha = 1$, U^A
212 approaches a proxy for sample absolute abundance itself. In ordination space (Fig. S3), this can
213 cause Axis 1 to correlate with absolute abundance and in some cases (freshwater and soil)
214 produces strong horseshoe effects [15], potentially distorting ecological interpretation. Beyond
215 tuning α to modify the influence of abundances, approaches such as NMDS or partial ordination
216 can also be used to modulate the sensitivity of ordinations to microbial load [16].

Deleted: [16]



219 *Figure 3. Discriminatory performance of U^A and related metrics across four microbial systems.* (A) PERMANOVAs
 220 were used to quantify the percent variance (R^2) explained by predefined categorical groups (shown in italics beneath
 221 each dataset name), with 1,000 permutations. PERMANOVA results were evaluated across five metrics and, where
 222 applicable, across eleven α values (0-1 in 0.1 increments). For consistency with the original studies, only samples
 223 from Reactor cycle 1 were used for the cooling-water dataset, only stool samples for the mouse gut dataset, and only
 224 mature rhizosphere samples for the [soil dataset](#) ([no samples were excluded from the freshwater dataset](#)). (B) Mantel
 225 correlation (R) between each distance metric and the pairwise differences in absolute abundance (cell counts or 16S
 226 copy number), illustrating the degree to which each metric is driven by biomass differences.

227 We recommend calibrating α based on research goals, modulating this effect by using
 228 GU^A across a range of α rather than relying on U^A ($\alpha = 1$). Researchers should consider how
 229 much emphasis they want their dissimilarity metric to place on microbial load (Box 1). When
 230 biomass differences are central to the hypothesis being tested (for example, detecting
 231 cyanobacterial blooms), high α are recommended. In contrast, if microbial load is irrelevant or
 232 independent of the hypothesis in question, low α (or U^R) may be preferred; for example in the
 233 soil dataset, fine-scale differences in composition may be obscured by random variation in
 234 microbial load.

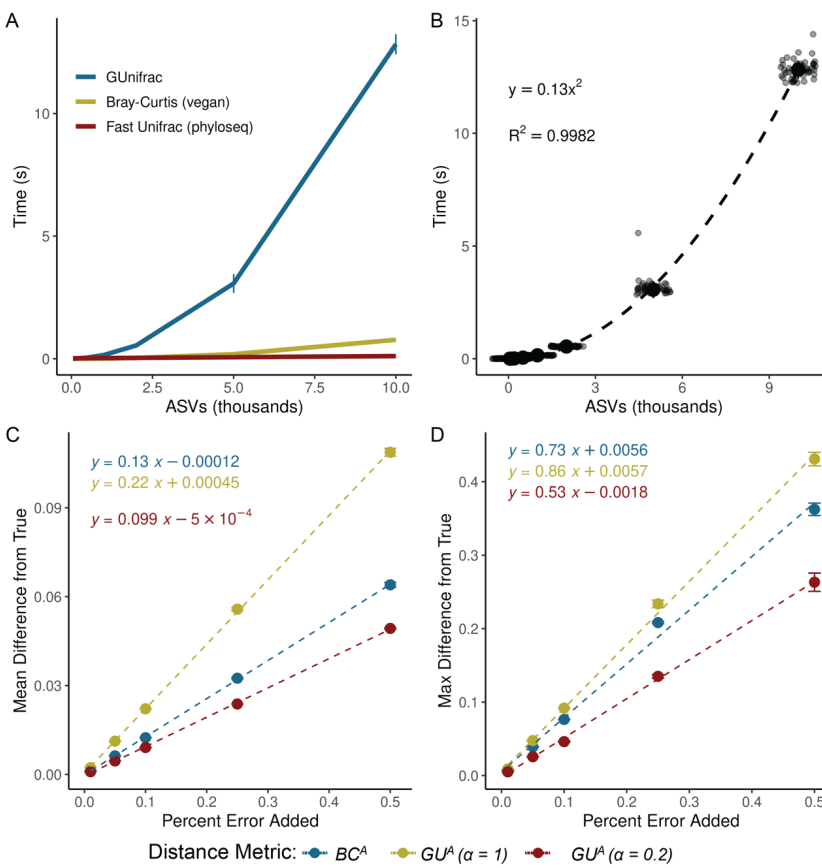
235 In many systems, microbial biomass is one piece of the story, likely correlated to other
 236 variables being tested. If the importance of microbial load in the system is unknown, one
 237 potential approach is to calculate correlations as demonstrated in Fig. 3B and select an α prior to
 238 any ordinations or statistical testing. Again, correlation to cell count is valuable and is intrinsic to
 239 absolute abundance-aware measures, especially when microbial load is relevant to the
 240 hypotheses being tested. Correlations to cell count in BC^A , an accepted approach in the literature,
 241 ranged from ~0.5 up to ~0.8. As a general recommendation from these analyses, we recommend
 242 α values in an intermediate range from 0.1 up to 0.6, wherein GU^A has similar correlation to cell
 243 count as BC^A .

244 Computational and Methodological Considerations

245 [Applying \$GU^A\$ in practice raises several considerations related to sequencing depth,](#)
 246 [richness, and computational cost. Both Bray-Curtis and UniFrac can be sensitive to sequencing](#)
 247 [depth because richness varies with read count \[17–19\]. To address this, we provide a workflow](#)
 248 [and accompanying code describing how we incorporated rarefaction into our own analyses \(Box](#)

249
250 2; available code). This approach minimizes sequencing-depth biases while preserving
abundance scaling for downstream β -diversity analysis.

251 To explore the sensitivity of GU^A to rarefaction, we calculated GU^A using rarefaction at
252 multiple sequencing depths, and used Mantel tests to assess the correlation between the rarefied
253 GU^A distance matrices the non-rarefied control (Fig. S4; supplemental methods). GU^A was
254 largely insensitive to rarefaction at high α values, even at depths as low as 250 reads per sample,
255 but sensitivity increased as α decreased (Fig. S4). When rarefying to the minimum sequencing
256 depth, as recommended, the effect of rarefaction was negligible (all Mantel's R > 0.95, Fig. S4).



257
258 *Figure 4. GU^A requires more computational time but remains resilient to quantification error. (A) Runtime for GU^A*
259 (*GUUnifrac package*), U^R (*FastUniFrac* in the *phyloseq* package) and BC^A (*vegan* package) was benchmarked across
260 50 iterations on a sub-sampled soil dataset (mature samples only) [10], using increasing ASV richness (50, 100, 200,
261 500, 1,000, 2,000, 5,000, 10,000), with 10 samples and one α value per run (unweighted UniFrac is also calculated
262 by default). Error bars represent standard deviation. (B) Quadratic relationship between GU^A computation time and
263 ASV richness. Large center point represents median across 50 iterations, error bars (standard deviation) are too

Deleted: Applying GU^A in practice raises several considerations related to sequencing depth, richness, and computational cost. Both Bray-Curtis and UniFrac can be sensitive to sequencing depth because richness varies with read count [17–19]. Methods to address these concerns, including rarefaction, remain debated and are challenging to benchmark rigorously [19]. We do not evaluate the sensitivity of U^A or GU^A to different rarefaction strategies here, but we do provide a workflow and code for how we incorporated rarefaction into our own analyses (Box 2 and available code). This approach minimizes sequencing-depth biases while preserving abundance scaling for downstream β -diversity analysis.

277 small to be seen. All benchmarks were run on an AMD EPYC 64-core processor with 1014 GB system memory (R
278 v4.3.3, vegan v2.7-1, phyloseq v1.52.0, GUnifrac v1.8.1). (C-D) Sensitivity of GU^A ($\alpha = 1$ and 0.2) and BC^A to
279 measurement error was evaluated by adding random variation ($\pm 1\%$ to $\pm 50\%$; Supporting Methods) to 16S copy
280 number estimates in stool samples from the mouse gut dataset [3]. For each error level, 50 replicate matrices were
281 generated and compared to the original values. Panels reflect the (C) mean difference and (D) max difference
282 between the error-added metrics compared to the originals. Error bars represent the standard deviation of the average
283 mean and max difference across 50 iterations.

Deleted:

284 GU^A is slower to compute than both BC^A and U^R because it must traverse the phylogenetic
285 tree to calculate branch lengths for each iteration. Computational time of GU^A increases
286 quadratically with ASV number and is 10-20 times slower, though up to 50 times slower, than
287 BC^A (Fig. 4A-B). The number of samples or α values, however, have relatively little effect on
288 runtime (Fig. S5). For a dataset of 24,000 ASVs, computing on a single CPU is still reasonable
289 (1.4 minutes), but repeated rarefaction increases runtime substantially because branch lengths are
290 redundantly calculated with each iteration. Allowing branch-length objects to be cached or
291 incorporated directly into the GUnifrac workflow would considerably improve computational
292 efficiency.

Deleted: Fig. S4

293 We also evaluated the sensitivity of GU^A to measurement error in absolute abundance due
294 to uncertainty arising from the quantification of cell number or 16S copy number. To assess the
295 sensitivity of GU^A and BC^A to measurement error, we added random error to the 16S copy
296 number measurements from the mouse gut dataset, limiting our analyses to the stool samples
297 where copy numbers varied by an order of magnitude. Across 50 iterations, each copy number
298 could randomly vary by a given percentage of error in either direction. We re-calculated β -
299 diversity (BC^A and GU^A at $\alpha = 1$ and $\alpha = 0.2$) and compared these measurements to the original
300 dataset.

Deleted: f

301 Introducing random variation into measured 16S copy number altered GU^A values only
302 modestly, and the effect was proportional to the magnitude of the added noise (Fig. 4C-D). At α
303 = 1, each 1% of quantification error introduced an average difference of 0.0022 in GU^A ; at $\alpha =$
304 0.2, GU^A was even less sensitive. Thus, moderate α values provide a balance between
305 interpretability and robustness to noise in absolute quantification. The max deviation from true
306 that added error could inflict on a given metric was also proportional (and always less) than the
307 magnitude of the error itself (Fig. 4D). A more rigorous approach to assessing error propagation
308 within these metrics, including mathematical proofs of the relationships estimated above, is
309 outside the scope of this paper but would be helpful.

310 GU^A was also insensitive to normalization approaches that adjust ASV abundances based
311 on the predicted 16S rRNA gene copy number (Fig. S6; supplemental methods). We used
312 PICRUSt2 (v2.6) to normalize ASV abundances within each dataset based on predicted 16S copy
313 number per genome, and then applied our standard rarefaction pipeline prior to GU^A calculation
314 (Box 2) [20, 21]. Correlations between GU^A distance matrices calculated from 16S copy number-
315 normalized datasets and those from the original, non-normalized datasets were consistently near
316 unity across all datasets (Mantel's R > 0.98, Fig. S6A), demonstrating that 16S copy number-
317 normalization had a negligible effect on GU^A . Sensitivity of GU^A to 16S copy number-
318 normalization generally decreased with increasing values of α in the cooling reactor, freshwater,
319 and soil datasets, but not in the mouse gut dataset (Fig. S6A). In the mouse gut dataset, several
320 highly abundant ASVs belonging to the genus *Faecalibaculum* had predicted 16S copy numbers
321 of seven copies per genome, explaining the relatively greater (though still weak) sensitivity of

325 this dataset to copy number-normalization (Fig. S6B). Finally, we note that 16S copy number-
326 normalization does not account for variation in genome copies per cell (ploidy), which can vary
327 across several orders of magnitude between species and growth phase [22–24].

328 Ecological Interpretation and conceptual significance

Deleted: [20, 21][22–24]

329 Absolute UniFrac reframes the interpretation of β -diversity by making biomass an explicit
330 ecological axis rather than an unmeasured or normalized-away quantity. Conventional UniFrac
331 captures composition and shared evolutionary history, but implicitly invites interpretation as if it
332 also encodes differences on microbial load. By incorporating absolute abundance directly,
333 Absolute UniFrac helps to resolve this mismatch and restores alignment between ecological
334 hypotheses and the quantities represented in the metric. In this view, β -diversity becomes a three-
335 axis ecological measure, incorporating composition, phylogeny and biomass, rather than a two-
336 axis approximation. That said, the additional dimension of microbial load also increases the
337 complexity of applying and interpreting this metric.

Deleted: ,

338 There are many cases where the incorporation of absolute abundance allows microbial
339 ecologists to assess more realistic, ecologically-relevant differences in microbial communities,
340 especially when microbial load is mechanistically central. Outside of the datasets re-analyzed
341 here [3, 5, 9, 10]; the temporal development of the infant gut microbiome involves both a rise in
342 absolute abundance and compositional changes [6]; bacteriophage predation in wastewater
343 bioreactors can be understood only when microbial load is considered [25]; and antibiotic-driven
344 declines in specific swine gut taxa were missed using relative abundance approaches [26]. As β -
345 diversity metrics (and UniFrac specifically) remain central to microbial ecology, these findings
346 highlight how interpretation changes once biomass is incorporated. Broader adoption of absolute
347 abundance profiling will also depend on data availability. Few studies currently make absolute
348 quantification data publicly accessible, underscoring the need to deposit absolute measurements
349 alongside sequencing reads for reproducibility, ideally as metadata within SRA submissions.

350 While demonstrated here with 16S rRNA data, the approach should extend to other marker
351 genes or (meta)genomic features, provided absolute abundance estimates are available. In this
352 sense, GU^A offers a more ecologically grounded view of lineage turnover by jointly reflecting
353 variation in biomass and phylogenetic structure.

354 No single metric (or α in GU^A), however, is universally “best”. Each β -diversity metric
355 emphasizes a different dimension of community change. Researchers should therefore select
356 metrics based on the ecological quantity that is hypothesized to matter most (Box 1). Here, we
357 demonstrate not that GU^A outperforms other measures, but that it faithfully incorporates the three
358 axes of variation it was designed to incorporate: composition, phylogenetic similarity, and
359 absolute abundance (Fig. 1 and Fig. 2). As with any β -diversity analysis, interpretation requires
360 matching the metric to the ecological question at hand, and exploring sensitivity across different
361 metrics where appropriate [27]. By providing demonstrations and code for the application and
362 interpretation of U^A/GU^A , we hope to encourage the use of these metrics as a tool of microbial
363 ecology.

364 Conclusion

365 By explicitly incorporating absolute abundance, Absolute UniFrac shifts phylogenetic β -
366 diversity from a two-axis approximation to a three-axis ecological measure. This reframing

369 connects the metric to the underlying biological questions that motivate many microbiome
370 studies. As methods for quantifying microbial load continue to expand, the ability to interpret β -
371 diversity in a biomass-aware framework will become increasingly important for distinguishing
372 true ecological turnover from proportional change alone. In this way, Absolute UniFrac is not
373 simply an alternative distance metric but a tool for aligning statistical representation with
374 ecological mechanism.

375

377 **Box 1: β -diversity metrics should reflect the hypothesis being tested**

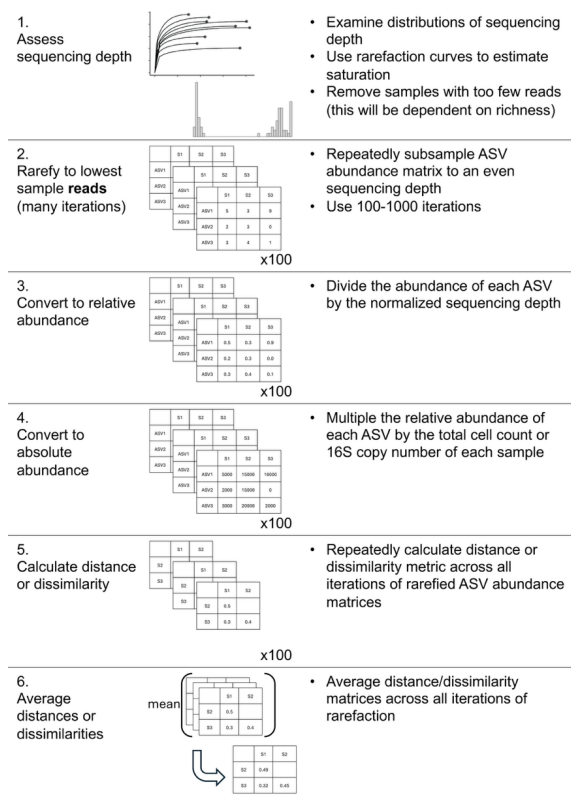
378 Absolute UniFrac is most informative when variation in microbial load is expected to carry
 379 ecological meaning rather than being a nuisance variable. The choice of α determines how
 380 strongly abundance differences influence the metric, and should therefore be selected based on
 381 the hypothesis, not by convention. In settings where biomass is central to the mechanism under
 382 study, higher α values appropriately foreground that signal, whereas in cases where load
 383 variation is incidental or confounding, lower α values maintain interpretability. Framing α as a
 384 hypothesis-driven choice repositions β -diversity from a default normalization step to an explicit
 385 ecological decision.

			Central to hypothesis			Metric to Use	Hypothetical Example	
Treat closely related lineages as similar?	Yes	How relevant is microbial load?	Relevant, but associated with other variables of interest			$GU^A, \alpha > 0.5$	Cyanobacterial bloom, pathogen proliferation	
			Irrelevant	Emphasize rare or dominant taxa?	Dominant	$GU^A, 0.1 < \alpha < 0.5$	Compositional shifts in response to nutrient addition	
					Rare	$GU^R, \alpha < 0.5$	Diet-associated microbiome shifts across hosts	
			Unknown			GU^A at multiple α	Tributary inputs of rare taxa	
	No	Microbial load relevant?	Yes			BC^A	Random variation in microbial load obscured compositional shifts in soil communities	
			No			BC^R	Strain turnover and proliferation in the infant gut	
						Temporal succession in chemostat		

389 Box 2: Rarefaction workflow for incorporating absolute abundance

While we refrain from an in-depth analysis of rarefaction approaches, here we present our workflow for incorporating rarefaction alongside absolute abundance. First, samples were assessed for anomalously low read counts and discarded (sequencing blanks and controls were also removed). For rarefaction, each sample in the ASV table was subsampled to equal *sequencing* depth (# of reads) across 100 iterations, creating 100 rarefied ASV tables. These tables were then converted to relative abundance by dividing each ASV's count by the equal sequencing depth (rounding was not performed). Then, each ASV's absolute abundance within a given sample was calculated by multiplying its relative abundance by that sample's total cell count or 16S copy number. Methods to predict genomic 16S copy number for a given ASV were not used unless explicitly stated (Fig. S6) [20].

415 unless explicitly stated (Fig. S6) [20, 21]. Each distance/dissimilarity metric was then calculated
416 across all 100 absolute-normalized ASV tables. The final distance/dissimilarity matrix was
417 calculated by averaging all 100 iterations of each distance/dissimilarity calculation. Of note for
418 future users: pruning the phylogenetic tree after rarefaction for each iteration is not necessary –
419 ASVs removed from the dataset do not contribute nor change the calculated UniFrac
420 distances.



422

423

424 **References**

- 425 1. Gloor GB et al. Microbiome Datasets Are Compositional: And This Is Not Optional. *Front
Microbiol* 2017;8:2224. <https://doi.org/10.3389/fmicb.2017.02224>
- 426 2. Vandeputte D et al. Stool consistency is strongly associated with gut microbiota richness
and composition, enterotypes and bacterial growth rates. *Gut* 2016;65:57–62.
<https://doi.org/10.1136/gutjnl-2015-309618>
- 427 3. Barlow JT, Bogatyrev SR, Ismagilov RF. A quantitative sequencing framework for absolute
abundance measurements of mucosal and luminal microbial communities. *Nat Commun*
2020;11:2590. <https://doi.org/10.1038/s41467-020-16224-6>
- 428 4. Wang X et al. Current Applications of Absolute Bacterial Quantification in Microbiome
Studies and Decision-Making Regarding Different Biological Questions. *Microorganisms*
2021;9:1797. <https://doi.org/10.3390/microorganisms9091797>
- 429 5. Props R et al. Absolute quantification of microbial taxon abundances. *ISME J* 2017;11:584–
587. <https://doi.org/10.1038/ismej.2016.117>
- 430 6. Rao C et al. Multi-kingdom ecological drivers of microbiota assembly in preterm infants.
Nature 2021;591:633–638. <https://doi.org/10.1038/s41586-021-03241-8>
- 431 7. Bray JR, Curtis JT. An Ordination of the Upland Forest Communities of Southern
Wisconsin. *Ecological Monographs* 1957;27:326–349. <https://doi.org/10.2307/1942268>
- 432 8. Lozupone CA et al. Quantitative and Qualitative β Diversity Measures Lead to Different
Insights into Factors That Structure Microbial Communities. *Applied and Environmental
Microbiology* 2007;73:1576–1585. <https://doi.org/10.1128/AEM.01996-06>

- 445 9. Pendleton A, Wells M, Schmidt ML. Upwelling periodically disturbs the ecological
446 assembly of microbial communities in the Laurentian Great Lakes. 2025. bioRxiv, 2025. ,
447 2025.01.17.633667
- 448 10. Zhang K et al. Absolute microbiome profiling highlights the links among microbial
449 stability, soil health, and crop productivity under long-term sod-based rotation. *Biol Fertil
450 Soils* 2022;58:883–901. <https://doi.org/10.1007/s00374-022-01675-4>
- 451 11. Chen J et al. Associating microbiome composition with environmental covariates using
452 generalized UniFrac distances. *Bioinformatics* 2012;28:2106–2113.
453 <https://doi.org/10.1093/bioinformatics/bts342>
- 454 12. Lozupone C, Knight R. UniFrac: a New Phylogenetic Method for Comparing Microbial
455 Communities. *Applied and Environmental Microbiology* 2005;71:8228–8235.
456 <https://doi.org/10.1128/AEM.71.12.8228-8235.2005>
- 457 13. McMurdie PJ, Holmes S. phyloseq: An R package for reproducible interactive analysis and
458 graphics of microbiome census data. *PLoS ONE* 2013;8:e61217.
- 459 14. Bolyen E et al. Reproducible, interactive, scalable and extensible microbiome data science
460 using QIIME 2. *Nat Biotechnol* 2019;37:852–857. [https://doi.org/10.1038/s41587-019-0209-9](https://doi.org/10.1038/s41587-019-
461 0209-9)
- 462 15. Morton JT et al. Uncovering the Horseshoe Effect in Microbial Analyses. *mSystems*
463 2017;2:10.1128/msystems.00166-16. <https://doi.org/10.1128/msystems.00166-16>
- 464 16. Paliy O, Shankar V. Application of multivariate statistical techniques in microbial ecology.
465 *Molecular Ecology* 2016;25:1032–1057. <https://doi.org/10.1111/mec.13536>

- 466 17. Schloss PD. Evaluating different approaches that test whether microbial communities have
467 the same structure. *The ISME Journal* 2008;2:265–275.
468 <https://doi.org/10.1038/ismej.2008.5>
- 469 18. Fukuyama J et al. Comparisons of distance methods for combining covariates and
470 abundances in microbiome studies. *Biocomputing 2012*. WORLD SCIENTIFIC, 2011,
471 213–224.
- 472 19. McMurdie PJ, Holmes S. Waste Not, Want Not: Why Rarefying Microbiome Data Is
473 Inadmissible. *PLOS Computational Biology* 2014;10:e1003531.
474 <https://doi.org/10.1371/journal.pcbi.1003531>
- 475 20. Wright RJ, Langille MGI. PICRUSt2-SC: an update to the reference database used for
476 functional prediction within PICRUSt2. *Bioinformatics* 2025;41:btaf269.
477 <https://doi.org/10.1093/bioinformatics/btaf269>
- 478 21. Douglas GM et al. PICRUSt2 for prediction of metagenome functions. *Nat Biotechnol*
479 2020;38:685–688. <https://doi.org/10.1038/s41587-020-0548-6>
- 480 22. Griesse M, Lange C, Soppa J. Ploidy in cyanobacteria. *FEMS Microbiol Lett* 2011;323:124–
481 131. <https://doi.org/10.1111/j.1574-6968.2011.02368.x>
- 482 23. Mendell JE et al. Extreme polyploidy in a large bacterium. *Proceedings of the National
483 Academy of Sciences* 2008;105:6730–6734. <https://doi.org/10.1073/pnas.0707522105>
- 484 24. Pecoraro V et al. Quantification of Ploidy in Proteobacteria Revealed the Existence of
485 Monoploid, (Mero-)Oligoploid and Polyploid Species. *PLOS ONE* 2011;6:e16392.
486 <https://doi.org/10.1371/journal.pone.0016392>

- 487 25. Shapiro OH, Kushmaro A, Brenner A. Bacteriophage predation regulates microbial
488 abundance and diversity in a full-scale bioreactor treating industrial wastewater. *The ISME
489 Journal* 2010;4:327–336. <https://doi.org/10.1038/ismej.2009.118>
- 490 26. Wagner S et al. Absolute abundance calculation enhances the significance of microbiome
491 data in antibiotic treatment studies. *Front Microbiol* 2025;**16**.
492 <https://doi.org/10.3389/fmicb.2025.1481197>
- 493 27. Kers JG, Saccenti E. The Power of Microbiome Studies: Some Considerations on Which
494 Alpha and Beta Metrics to Use and How to Report Results. *Front Microbiol* 2022;**12**.
495 <https://doi.org/10.3389/fmicb.2021.796025>
- 496